Letters

Research on Common Mode EMI and Its Reduction for Active Magnetic Bearings

Yuanhao Xie, *Graduate Student Member, IEEE*, Dong Jiang, *Senior Member, IEEE*, Feng Hu, *Student Member, IEEE*, and Zicheng Liu, *Senior Member, IEEE*

***Abstract*—Active magnetic bearing (AMB) with power electronics drive is an important technology for high-speed rotational machinery suspension. There were seldom literatures concerning the common mode (CM) electromagnetic interference (EMI) problems of the AMB system. In this article, we found that the power electronic converter used for AMB control will not only bring EMI to the devices but also influence the performance of the levitation control. To cope with this problem, the parasitic paths of the leakage currents in the five-degrees-of-freedom AMB system were analyzed. The control principle and the novel zero CM PWM (ZCMPWM) strategy for the AMB driven by a four-leg converter were presented to suppress the CM EMI. Experiment has been done on an AMB-based compressor. The proposed method can significantly reduce the CM EMI caused by the AMB controller and improve the performance of levitation.**

***Index Terms*—Active magnetic bearing (AMB), common mode (CM) electromagnetic interference, modulation.**

I. Introduction

ACTIVE magnetic bearing (AMB) is an advanced kind of bearing device for rotating machinery. The electromagnet with controllable winding current is used to produce the reluctance force to achieve levitation. Since there is no contact between the rotor and stator, it has the unique characteristics including zero friction, much less maintenance and lubrication requirement, long working life as well as low vibration noise. These advantages make the AMB the better choice for a high-speed rotating equipment as well as advanced drive systems, including flywheel, turbomachinery, aerospace actuator, and so on [1].

A typical radial 2-D AMB system is shown in Fig. 1. The eight magnetic poles can generate forces in both x- and y-axes.

Manuscript received 23 October 2022; revised 3 December 2022; accepted 5 January 2023. Date of publication 10 January 2023; date of current version 14 February 2023. This work was supported in part by the National Natural Science Foundation of China (NSFC) under Grant U1866211. *(Corresponding author: Dong Jiang.)*

The authors are with the State Key Laboratory of Advanced Electromagnetic Engineering and Technology, School of Electrical and Electronic Engineering, Huazhong University of Science and Technology, Wuhan 430074, China (e-mail: xieyh@hust.edu.cn; jiangd@hust.edu.cn; fenghu@hust.edu.cn; liuzc@hust.edu.cn).

Color versions of one or more figures in this article are available at https://doi.org/10.1109/TPEL.2023.3235775.

Digital Object Identifier 10.1109/TPEL.2023.3235775

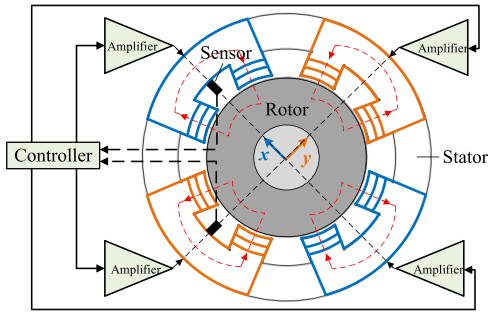

Fig. 1. Typical 2-D AMB system.

The opposite two magnets together form a pair of differential magnets to generate forces in opposite directions.

The displacement of the rotor is measured usually using an eddy current sensor. The reference currents for the four electromagnets are generated by the position controller and realized by four power amplifiers. Generally, the rotor has five-degrees-of-freedom (5-DOF), thus, two of the abovementioned systems are needed to control the radial movement, and an additional thrust AMB is needed to control the axial movement [1].

Serving as the key component of the AMB system, the power amplifier is usually a power electronic converter driven by PWM signals. The high-frequency switch action will cause a rapid change in bridge voltages which will eventually bring electromagnetic interference (EMI) to the system. While the differential mode (DM) current flows in the already existing circuit path, the common mode (CM) voltage will cause leakage current through the parasitic path.

The influence of the CM EMI has been widely studied in the field of grid-connected photovoltaic (PV) system and motor drive system. The CM leakage current will accelerate the aging of PV panels, causing shaft voltage and bearing current for the motor. Plenty amount of literatures have also concentrated on the suppression methods of the CM EMI [2], [3], [4]. Adding CM choke or *RLC* filter as well as Y-capacitors to the system are the passive ways. Emerging approaches including active EMI filters and zero CM PWM (ZCMPWM) methods have also been proposed.

However, to the extent of the knowledge of the authors, there is hardly any literature concentrating on the CM EMI problems

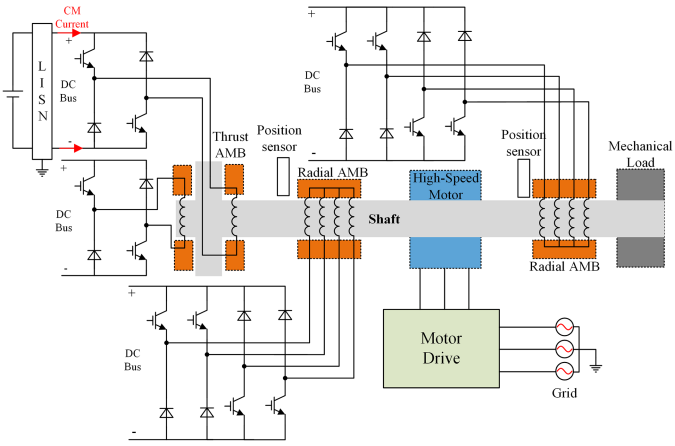

Fig. 2. System structure of the 5-DOF AMB with high-speed motor.

in the AMB system. Different from other kinds of power electronics applications, AMB is a multiaxis system coupled with the rotor shaft, and the EMI issue will be more complex. Also, the position sensors are critical components in the AMB system and easy to be influenced by EMI.

Thus, the research purposes of this article mainly consist of the following three key problems: First, to analyze the conduction model of the CM leakage currents in the AMB system; second, to research the influence of the CM EMI on the AMB system; third, to propose the CM EMI reduction method for AMB systems.

To achieve these purposes, the parasitic path of the leakage currents is analyzed in Part II. The control principle and the ZCMPWM strategy are proposed in Part III. The experiments are carried out in Part IV to show the influence of the CM EMI and validate its reduction method.

II. AMB System Structure and CM Equivalent Circuits

A typical 5-DOF AMB system is shown in Fig. 2. The 5-DOF levitation system can be divided into two radial and one axial AMBs (the three bearing parts). The power amplifier of the three parts shares the same dc bus. The voltages added to the windings of each specific bearing part have the same parasitic path due to the symmetry of the windings, but this symmetry characteristic is no longer visible when considering the windings between two different bearing parts because of the different installation conditions. Two points can be gotten from these characteristics. One is that the CM voltage (CMV) of each bearing part should be defined as the average of all the voltages added to the windings as presented in the following:

$$V_{\mathrm{CM}} = \frac{1}{n}\sum_{i=1}^{n} V_i. \tag{1}$$

Another is that when designing ZCMPWM strategy for the 5-DOF AMB system, the CMV of each bearing part should be suppressed separately.

Before analyzing the CM EMI in the AMB system, it is essential to decide the circuit topology of the AMB power amplifier. Full H-bridge topology is typically used as power amplifier. Since this type of converter always has an even number of bridge

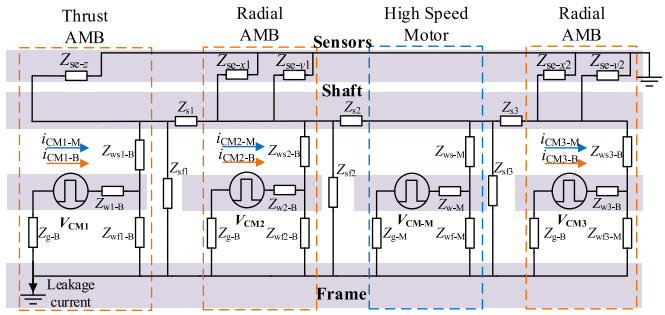

Fig. 3. Lumped parameter equivalent circuit of the CM parasitic path.

legs, it is possible to eliminate the CMV by connecting half of the bridge legs to the positive dc bus at any moment. However, the full H-bridge requires a large number of power electronic devices, resulting in a larger size and higher cost of the controller. From this point of view, many novel topologies have been proposed in recent years to optimize the number of switching devices, including shared-bridge converter [5], series winding converter [6], four-leg converter [7], and so on. Among them, the four-leg converter has the least number of switching devices, and the even number of bridge legs maintains the possibility of eliminating the CMV for radial AMBs. Therefore, two four-leg converters are chosen to drive the two radial magnetic bearings and two half H-bridge are selected to drive the windings of the thrust bearing. The whole system structure is shown in Fig. 2. A line impedance stabilization network (LISN) is connected between the dc source and the converter to isolate the EMI from the source side.

Based on the 5-DOF AMB and its drive system, the conduction path of the CM EMI has been studied using lumped parameter modeling method, which is similar to the CM conduction path modeling of the traditional motor [8]. The simplified equivalent circuit of the CM parasitic path is shown in Fig. 3. The subscript B in this figure means AMB system and M means high-speed motor system, Z_{g} is the grounding impedance of the dc source, Z_{s} is the shaft impedance, Z_{ws} is the equivalent CM impedance between windings and shaft, Z_{wf} is the equivalent CM impedance between windings and the frame, and Z_{sf} is the impedance between shaft and the frame. It can be seen that all of the four power components will generate high-frequency CM excitation sources in the 5-DOF AMB system and they will influence each other so it is unwise to concentrate on the leakage current of each part separately. To eliminate the CM leakage current, all of the four CM sources need to be suppressed at the same time. This is a significant difference between the AMB system and the traditional motor drive system. Fortunately, what we are concerning is the CM EMI of the whole AMB controller. The total leakage current of the AMB system can be separated into two parts; one is caused by the AMB system itself; the other part is caused by the high-speed motor drive.

More important, the position sensor probes in the AMB system is coupled with the shaft with impedance of Z_{se} (for each axis) in Fig.3. The CM current in the shaft will easily impact the noise in the position sensors and highly interfere with the levitation precision, which will be evaluated in the experimental results part. EMI is a practical threat to AMB operation.

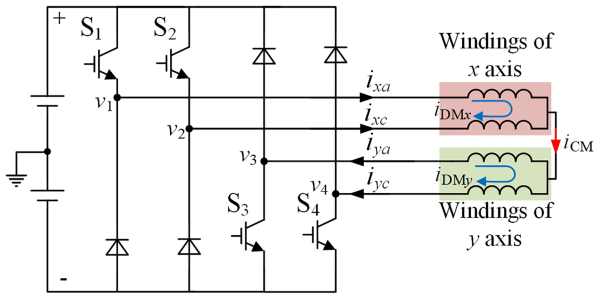

Fig. 4. Four-leg converter topology.

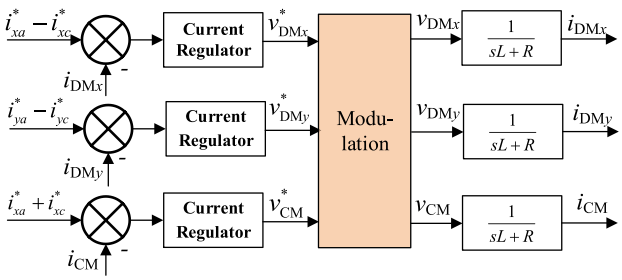

Fig. 5 Control diagram of the four-leg converter.

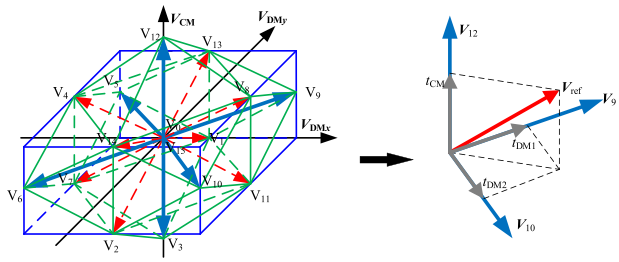

Fig. 6. Vector diagram of the ZCMPWM.

TABLE I
LIST OF THE ZCMVS

ZCMV	v_{CM}	$v_{\mathrm{DM}x}$	$v_{\mathrm{DM}y}$	Switching status
$\boldsymbol{V}_3$	$-V_{\mathrm{dc}}$	0	0	0011
$\boldsymbol{V}_5$	0	$-V_{\mathrm{dc}}$	V_{dc}	0101
$\boldsymbol{V}_6$	0	$-V_{\mathrm{dc}}$	$-V_{\mathrm{dc}}$	0110
$\boldsymbol{V}_9$	0	V_{dc}	V_{dc}	1001
$\boldsymbol{V}_{10}$	0	V_{dc}	$-V_{\mathrm{dc}}$	1010
$\boldsymbol{V}_{12}$	V_{dc}	0	0	1100

III. Control Principle and ZCMPWM Strategy

Reduction of the CM EMI in the 5-DOF AMB system is discussed in this section, and the radial AMB with four-leg converter is of major concern. The magnetic force of the AMB is controlled via the well-known bias-plus-differential current mode [1]. The two windings of the same DOF will flow the same and constant bias current. The position signal is measured and fed to the position controller, and the output of the position controller is set as the differential reference current of the two windings.

The four-leg converter and the winding connection are shown in Fig. 4. There are four windings but only three DOF of current control, thus, the bias currents of the two axis windings are set the same and the CM current i_{CM} should always be equal to $2I_{\mathrm{bias}}$. The $i_{\mathrm{DM}x}$ in Fig. 4 is defined as i_{xa}-i_{xc}, and $i_{\mathrm{DM}y}$ is i_{ya}-i_{yc}.

The control diagram is shown in Fig. 5, where L and R are the inductance and resistance of the windings. The three current variables $i_{\mathrm{DM}x}$, $i_{\mathrm{DM}y}$, i_{CM} are controlled independently to generate reference voltages. The three voltage variables are defined as

$$\begin{aligned} v_{\mathrm{DM}x} &= v_{L1} - v_{L2} = (v_1 - v_N) - (v_2 - v_N) = v_1 - v_2 \\ v_{\mathrm{DM}y} &= v_{L3} - v_{L4} = (v_N - v_3) - (v_N - v_4) = v_4 - v_3 \\ v_{\mathrm{CM}} &= v_{L1} + v_{L2} = v_1 - v_N + v_2 - v_N \\ &= (v_1 + v_2 - v_3 - v_4)/2 \end{aligned} \tag{2}$$

where v_{L1}, v_{L2}, v_{L3}, v_{L4} are the voltage across the four windings, v_1, v_2, v_3, v_4 are the voltages of the four legs as shown in Fig. 4, v_N is the voltage of the common connection point of the windings which is equal to the average voltage of the four legs.

The three voltage variables can be calculated for each switching state of the converter based on (2). Taking the three voltage variables as orthogonal coordinate axes, the vector diagram of the 16 switch states of the four legs can be drawn and shown in Fig. 6.

To eliminate the high-frequency CMV of the converter, two bridge arms should be connected to the positive dc bus at any time, while the other two arms are connected to the negative bus. There are six voltage vectors that meet this requirement as shown by blue arrows in Fig. 6, which are named as zero CM vectors (ZCMV). The six ZCMVs divide the whole space into eight areas, any voltage vector can be composed of the three adjacent vectors.

The switching status of the ZCMVs are listed in Table I, where 1 means the leg voltage is high level and 0 means low level. It can be seen that two switches will operate when switching from one vector to its adjacent vector. Since there are at most eight times of switching transitions within one switching period of the four-leg converter, we can arrange four times of vector switching, corresponding to five segments of vectors. In addition to the three vectors needed to compose the reference voltage, $\boldsymbol{V}_3$ and $\boldsymbol{V}_{12}$, the two opposite vectors, are used to form the zero vector to fill the remaining time, and finally get a five-segment modulation scheme. It should be noted that any two opposite vectors can be used to synthesize the zero vector, but $\boldsymbol{V}_3$ and $\boldsymbol{V}_{12}$ can ensure the symmetry in the x and y directions. Taking the reference voltage within the area of $\boldsymbol{V}_9$, $\boldsymbol{V}_{10}$, $\boldsymbol{V}_{12}$ as an example, the operation time of the three vectors is calculated according to Fig. 6, the rest time of the switching cycle is t_0. The voltages of the four bridge legs within one switching period using the proposed ZCMPWM are shown in Fig. 7(a). The two parts of the action time of $\boldsymbol{V}_{12}$ are combined, while the action time of V_3 is divided into two halves at the beginning and end of a switching cycle. The voltage waveforms using the traditional carrier-based PWM (CBPWM) is shown in Fig. 7(b). It can be seen that the CMV is eliminated by only using the ZCMVs to form the reference voltage.

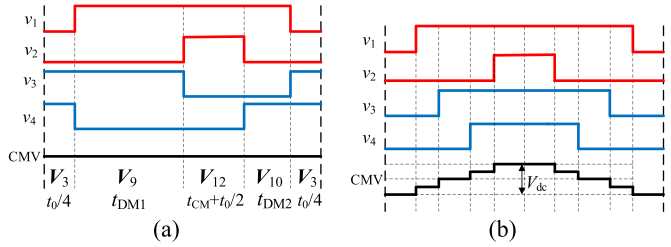

Fig. 7. Four-leg voltages of the converter with (a) ZCMPWM and (b) CBPWM.

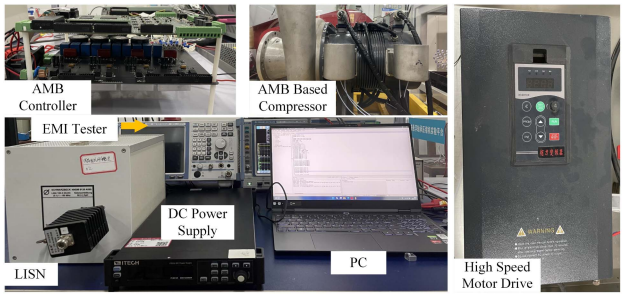

Fig. 8. Pictures of the experiment platform.

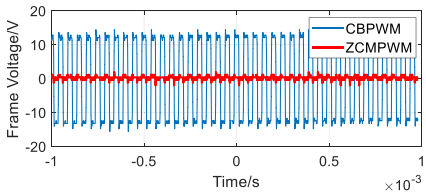

Fig. 9. Comparison of frame voltages.

With respect to the thrust AMB, each of the windings is controlled by half H-bridge whose control principle is well-documented in [9]. The freewheeling mode is canceled and the two switches are controlled to be ON or OFF at the same time to realize the zero CMV operation.

It should be noted that starting point of this article is the 5-DOF system, the proposed ZCMPWM strategy is also suitable for other types of multi-DOFs systems, for their control systems are the subsets of the 5-DOF system.

IV. Experiment Results

The remaining problems are how CM EMI and the proposed reduction method affect the AMB system. This is done by carrying out the experiments based on a 5-DOF AMB compressor prototype platform as shown in Fig. 8. The dc bus voltage of the AMB controller is 100 V, and its switching frequency is 20 kHz. The switching frequency of the motor drive is 4 kHz.

The system is first tested on the condition of static levitation to compare the traditional carrier-based PWM and the proposed ZCMPWM. The comparison of the frame voltages when the frame is not grounded is shown in Fig. 9. When the frame is grounded, the CM leakage current can be obviously observed as shown in Fig. 10. The EMI tester is used to test the CM EMI caused by the AMB controller, the results are shown in Fig. 11. It can be seen that the envelope of the CM EMI is reduced by

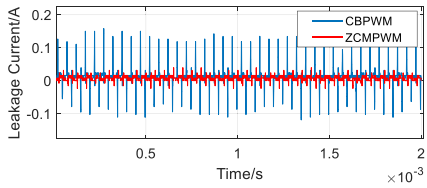

Fig. 10. Comparison of leakage currents.

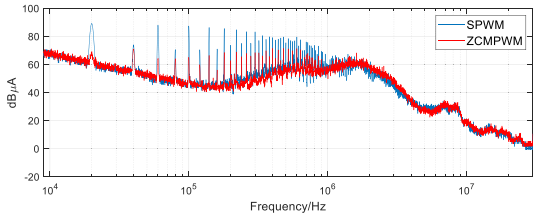

Fig. 11. CM EMI test results with static levitation.

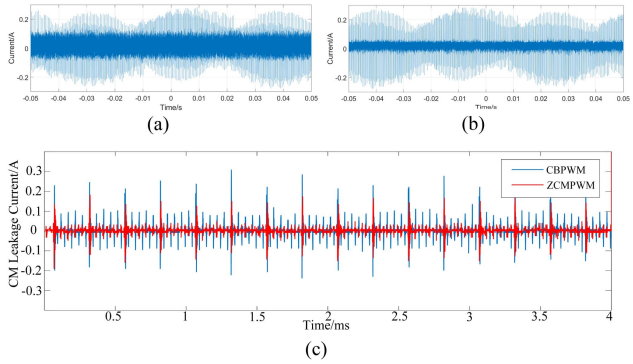

Fig. 12. Comparison of leakage currents when runs at 3000 r/min with (a) CBPWM, (b) ZCMPWM, (c) and zoom in.

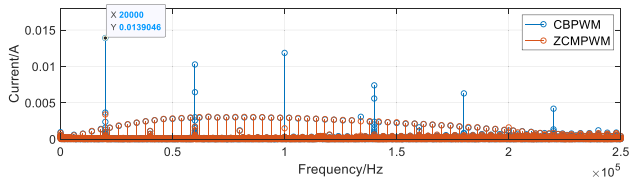

Fig. 13. FFT analysis results of the leakage current at 3000 r/min.

more than 20 dB when implementing the ZCMPWM. The three figures indicate that the CM noise is significantly reduced with the proposed ZCMPWM strategy. It should be noted that the EMI in the MHz band and above is mainly decided by the switching behavior of the power electronic devices [10], which would not be significantly affected by the modulation strategy.

Then, the motor drive is turned on and it runs the rotor to 3000 r/min, the CM leakage current of the AMB controller is shown in Fig. 12, and the FFT results are shown in Fig. 13. It can be seen that the CM leakage currents consist of two types of frequency components, the first part is the multiplication of the switching frequency of the AMB controller ($n\times$20 kHz), the second part is that of the motor drive ($n\times$4 kHz). This is the cross-coupling effect of the CM noise as previously analyzed. The first part can be well suppressed by the proposed ZCMPWM strategy, while the second part is unaffected. This phenomenon

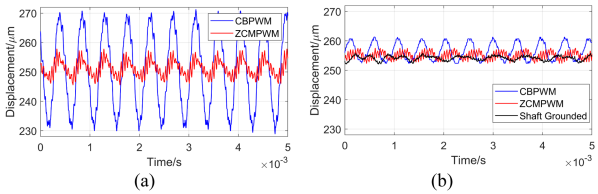

Fig. 14. Errors of the displacement sensor. (a) Ungrounded. (b) Grounded.

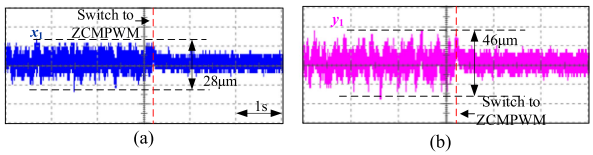

Fig. 15. Displacement signal of (a) x-axis and (b) y-axis under static levitation.

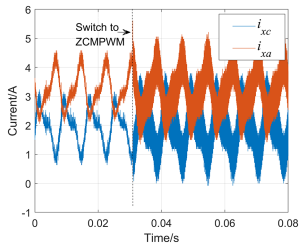

Fig. 16. Winding currents at 3000 r/min.

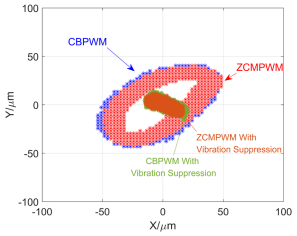

Fig. 17. Displacement at 3000 r/min.

indicates that the CM EMI suppression of the AMB controller and the motor drive can be decoupled.

Third, it is also important to study the influence of the CM EMI on the levitation control. First, following the principle of reducing the number of variables, the displacement signal of x direction is measured with the eddy current sensor, on condition that all the winding currents are controlled as 2.4 A and the shaft lies on the protection bearings and keeps stationary. The results are shown in Fig. 14.

It can be seen that the grounding of the frame can partly decrease the interference, while the suppression of the CM EMI will further reduce the error of the sensor. The high-frequency shaft voltage will serve as an interference source to the sensors as has been shown in Fig. 3, which can be reduced by both grounding of the frame and ZCMPWM strategy. Also, the grounding of the shaft can also achieve the same effect but can never be used in AMB systems.

This phenomenon has been further observed when the shaft is statically levitated and the frame is not grounded, the results are shown in Fig. 15. Moreover, when the rotor runs at 3000 r/min, the winding current of the x direction of one radial AMB is shown in Fig. 16 and the displacement signals are shown in Fig. 17. The vibration suppression algorithm used here refers to [11]. Although the current ripple is increased with the ZCMPWM, the displacement fluctuation will not deteriorate but will decrease slightly, because the displacement sensor error is reduced with ZCMPWM.

V. Conclusion

In this article, we focus on the CM EMI problem of the 5-DOF AMB system, which has seldom been mentioned in previous research. The system is driven by two novel four-leg converters and two half H-bridge converters. The whole system can be divided into four parts, which will produce four CM voltage sources, and their CM EMI will affect each other. A novel control and modulation strategy have been proposed to suppress the CM EMI of the AMB controller. In the experiment, it is found that the CM EMI suppression of the AMB controller and the motor drive can be decoupled. Another valuable conclusion is that the suppression of the CM EMI will reduce the error of the displacement sensor so as to realize a better performance of levitation. The ZCMPWM will cause greater ripples on winding currents but will not deteriorate the displacement control. This could be a starting point for the new research area of EMI of multiaxis AMB system.

References

[1] E. H. Maslen and G. Schweitzer, *Magnetic Bearings: Theory, Design, and Application to Rotating Machinery*. Berlin, Germany: Springer-Verlag, 2009.

[2] Z. Shen, D. Jiang, T. Zou, and R. Qu, "Dual-segment three-phase PMSM with dual inverters for leakage current and common-mode EMI reduction," *IEEE Trans. Power Electron.*, vol. 34, no. 6, pp. 5606–5619, Jun. 2019.

[3] D. Han, W. Lee, S. Li, and B. Sarlioglu, "New method for common mode voltage cancellation in motor drives: Concept, realization, and asymmetry influence," *IEEE Trans. Power Electron.*, vol. 33, no. 2, pp. 1188–1201, Feb. 2017.

[4] M. M. Jha, K. B. Naik, and S. P. Das, "Types of electro magnetic interferences in SMPS and using Y-capacitor for mitigation of mixed mode noise," in *Proc. IEEE Int. Conf. Power, Control Embedded Syst.*, 2010, pp. 1–6.

[5] C. Liu, Z. Deng, C. Hua, and K. Li, "Design and implementation of a five-phase six-leg switching power amplifier for five degrees of freedom magnetic levitation bearing system," in *Proc. IEEE 8th Conf. Ind. Electron. Appl.*, 2013, pp. 1254–1258.

[6] J. Yang, D. Jiang, H. Sun, A. Li, and Z. Liu, "Series-winding topology converter for active magnetic bearing drive," *IEEE Trans. Ind. Electron.*, vol. 68, no. 12, pp. 11772–11782, Dec. 2021.

[7] Z. Hu, D. Jiang, and H. Sun, "A four-phase four-leg power electronics converter for active magnetic bearing drive," *Trans. China Electrotechnical Soc.*, vol. 35, no. 20, pp. 4325–4335, 2020.

[8] F. Wang, "Motor shaft voltages and bearing currents and their reduction in multilevel medium-voltage PWM voltage-source-inverter drive applications," *IEEE Trans. Ind. Appl.*, vol. 36, no. 5, pp. 1336–1341, Sep./Oct. 2000.

[9] Y. Ren and J. Fang, "Current-sensing resistor design to include current derivative in PWM H-bridge unipolar switching power amplifiers for magnetic bearings," *IEEE Trans. Ind. Electron.*, vol. 59, no. 12, pp. 4590–4600, Dec. 2012.

[10] N. Oswald, P. Anthony, N. McNeill, and B. H. Stark, "An experimental investigation of the tradeoff between switching losses and EMI generation with hard-switched All-Si, Si-SiC, and All-SiC device combinations," *IEEE Trans. Power Electron.*, vol. 29, no. 5, pp. 2393–2407, May 2014.

[11] H. Sun, D. Jiang, and J. Yang, "Synchronous vibration suppression of magnetic bearing systems without angular sensors," *CES Trans. Elect. Mach. Syst.*, vol. 5, no. 1, pp. 70–77, 2021.